Modeling leaky faucet dynamics

A. D'Innocenzo* and L. Renna†
Dipartimento di Fisica dell'Università, 73100 Lecce, Italy
and Istituto Nazionale di Fisica Nucleare, Sezione di Lecce, 73100 Lecce, Italy
(Received 19 September 1996)

The variety of phenomena showed by a dripping faucet is interpreted in terms of simple one-dimensional relaxation oscillator models with different mechanisms of release of the drops. These models present most of the characteristic features of experimental data. Simulations are carried out, in order to link the parameters and the mechanisms of release of the models to the physical properties of the faucet. [S1063-651X(97)12506-5]

PACS number(s): 02.70.−c, 47.52.+j

I. INTRODUCTION

In recent years, there has been increasing interest in the study of dripping faucet dynamics. The suggestion that the drips falling from a leaky faucet might exhibit chaotic transitions as the flow rate is varied was first proposed by Rössler [1]. This prediction was experimentally confirmed afterwards by Shaw and co-workers [2,3]. Since then, the nonlinear behavior of a dripping faucet during the transition to chaos has been examined experimentally by several authors [4–10]. The broad range of dynamical behavior, including period doubling, hysteresis, and chaos, shown by the dripping faucet, is characteristic of a relaxation oscillator when internal oscillations are stimulated during the rapid transition after a threshold is reached, and may be found in many physical systems such as brakes engaged frictionally to a rotating shaft, electric relaxation oscillators, or magnetospheric substorms [11]. Thus the dripping faucet presents itself as a sort of ''guide system'' for modeling analog physical systems.

In the leaky tap, a continuous flow of water builds up until the drop, subjected to the weight and to the attractive force of the molecules, reaches a threshold point. Then a drop detaches and falls, stimulating a rebound and mechanical vibrations in the residual water, affecting the time of formation of the next drop. Thus the falling drop has influence on the motion of the next forming drop: the time intervals T_n between successive drop detachments become irregular or chaotic at certain values of flow rate.

As for the modeling of the dripping faucet dynamics, up to now the attempts made to explain the phenomena observed, as far as we know, are the variable-mass oscillator of Shaw [2,3], the electrical analog oscillator of Bernhardt [11], the one-dimensional feedback loop of Austin [8], and, recently, two different models [12,13] which improve upon Shaw's variable-mass oscillator.

The purpose of this work is to describe the results of investigations performed by using the modified oscillator models proposed in [13], to show the flexibility of these models and their capability of reproducing the characteristics of the dynamics of the leaky tap. In Ref. [13] only one of the models presented in this paper is analyzed, making two different suppositions about the mass of the drop breaking away. Conversely, in this paper two different mechanisms of rebound are compared with a single way of formation of the falling drop.

Our studies show that the models reproduce many qualitative features of the real system, and exhibit attractors very similar to those found experimentally. In particular, single and multiple closed-loop patterns, such as those reported in Ref. [5], are obtained; to our knowledge, these structures have not been reproduced by previous simulation models. Moreover, the evolution of the loop patterns (from a periodic state to a chaotic attractor) take place by distortion followed by folding, and this has an equivalent among the experiments for the actual dripping system.

In the final part of the paper a comparison is made between attractors obtained experimentally by us (using an experimental apparatus similar to that of Wu and Schelly [5]) and that obtained by simulation. Also from this analysis, a good qualitative agreement comes out between numerical and experimental attractors.

The paper is organized as follows. In Sec. II modeling of the dripping faucet dynamics is described, and in Sec. III dripping spectra at increasing flow rate are reported together with dripping time delay diagrams obtained at selected values of the flow rate. In Sec. IV results are discussed in connection with attractors obtained allowing variations of some model parameters. The capability of our models of reproducing some experimental data is shown in Sec. V. Finally, conclusions are drawn in Sec. VI.

II. SIMULATION MODELS

The behavior of the dripping faucet can be modeled as the one-dimensional motion of a variable mass M attached at a spring of elastic constant k, subjected to the gravitational force Mg and to a frictional force proportional to the speed v of the growing mass. The set of first-order differential equations of the model are [3]

*Electronic address: Dinno@le.infn.it
†Electronic address: Renna@le.infn.it

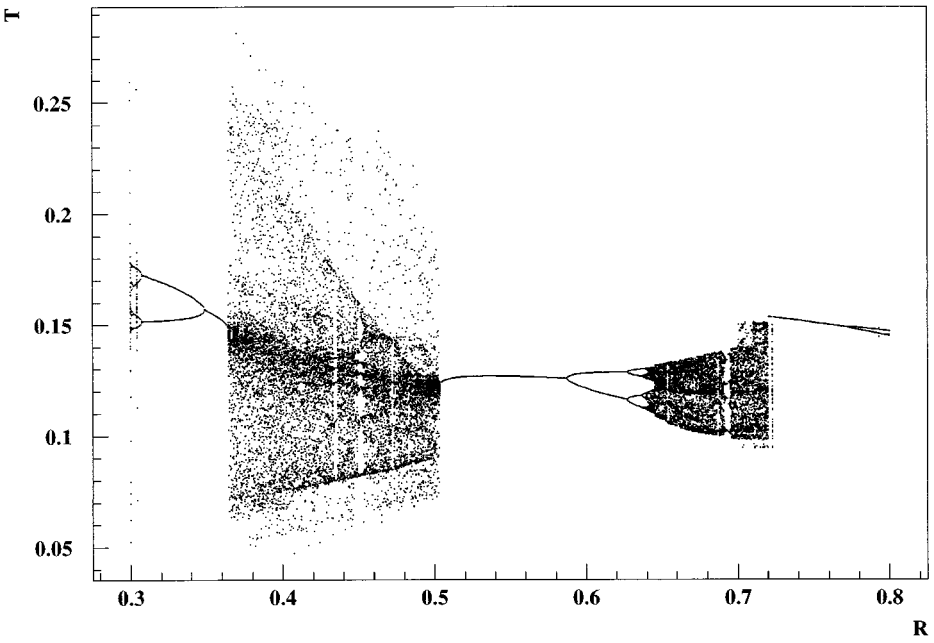

FIG. 1. PS dripping spectrum $[T(s)]$ plotted against flow rate R (g/s). The values of the parameters are: $g=980$ cm/s^2, $x_c=0.25$ cm, $k=475$ dyn/cm, $b=1$ g/s, and $\alpha=0.5$ s/cm; 50 points are used at each value of R, and 4×10^4 points for the whole plot.

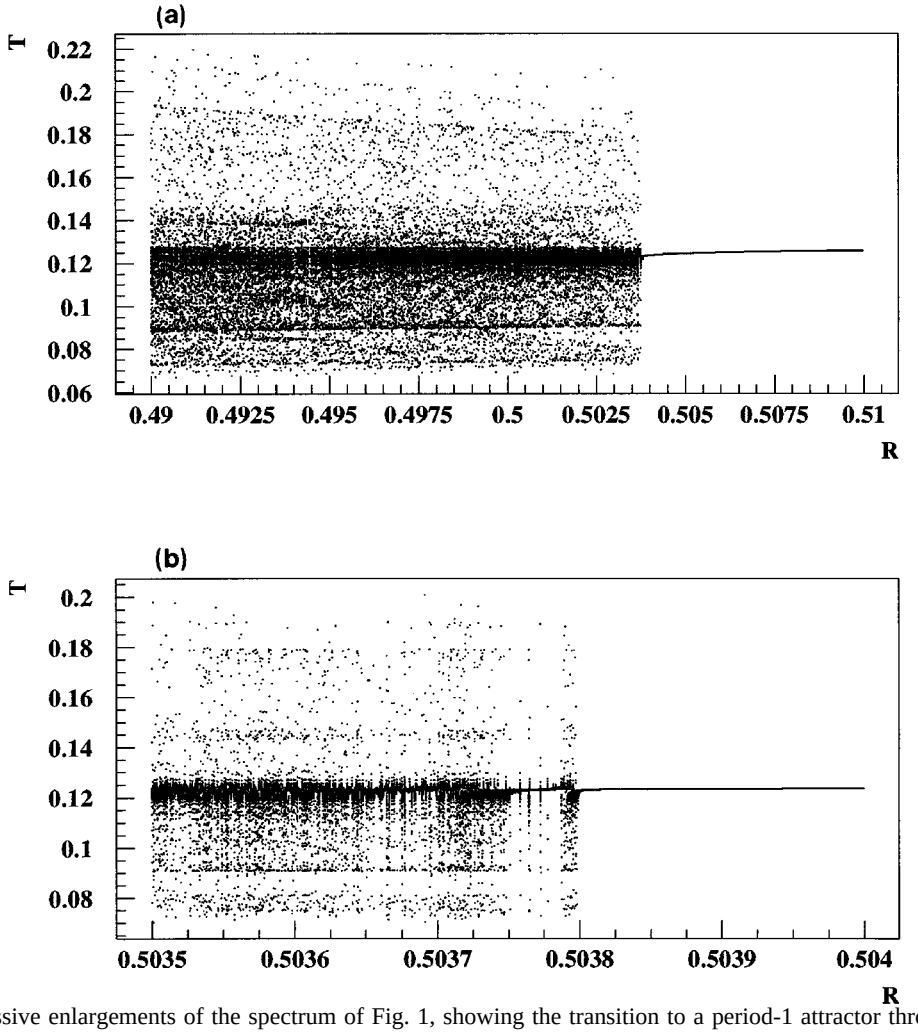

FIG. 2. Two successive enlargements of the spectrum of Fig. 1, showing the transition to a period-1 attractor through tangent intermittence. (Units as in Fig. 1.)

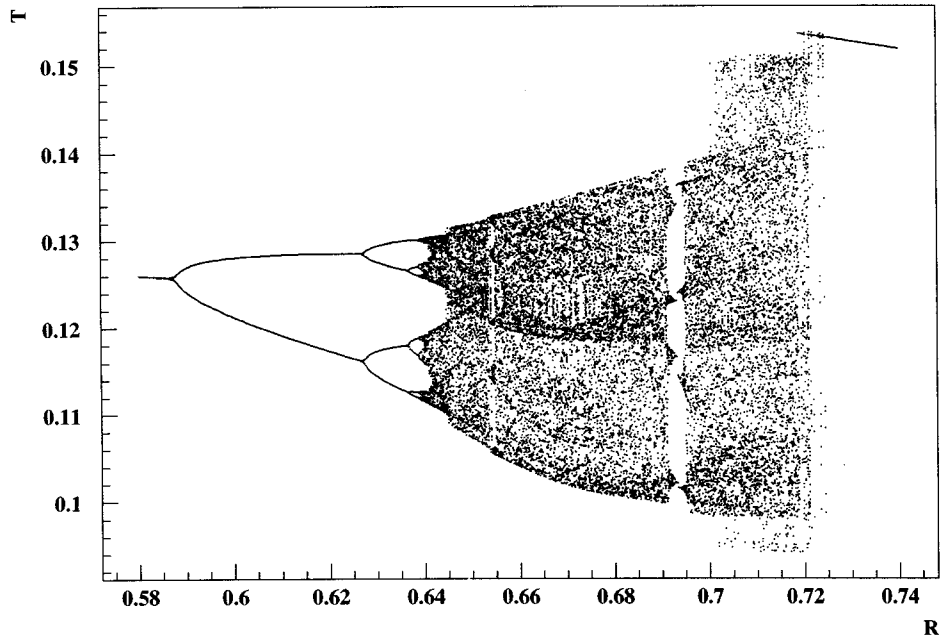

FIG. 3. An enlargement of a region of the spectrum of Fig. 1 showing a period-doubling route to chaos (units as in Fig. 1.)

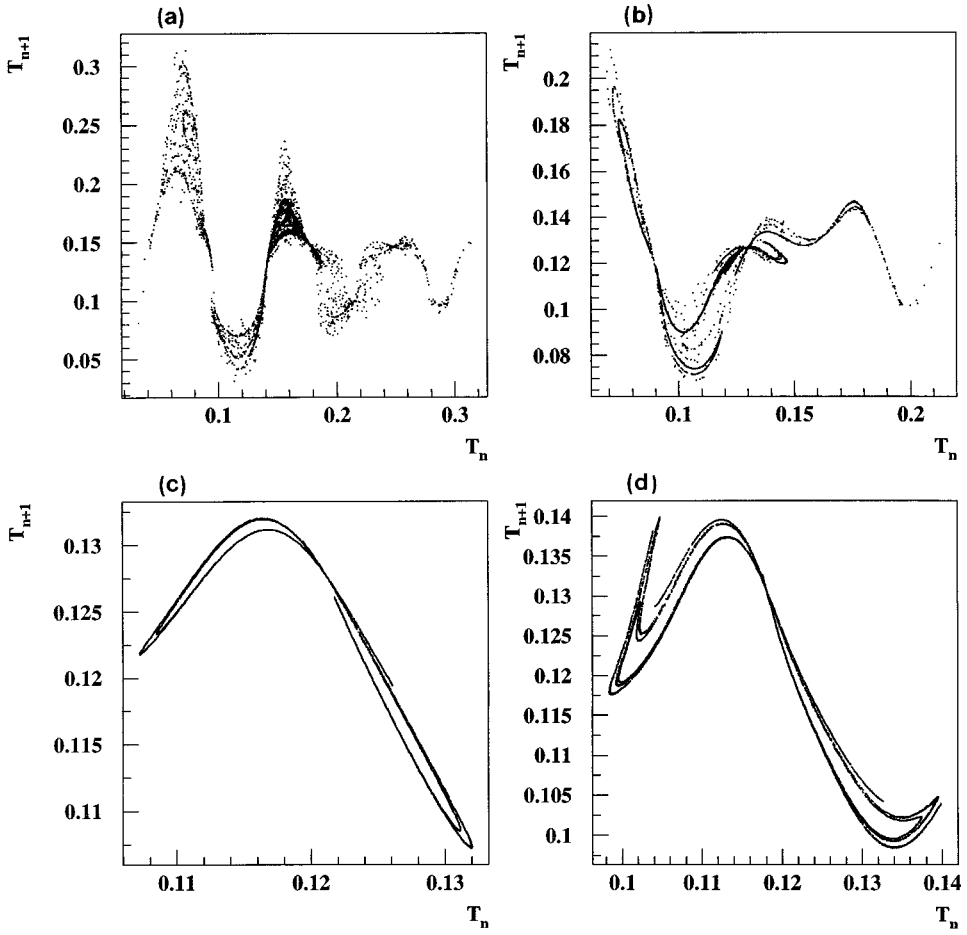

FIG. 4. Dripping time [T_n (s)] delay diagrams for (a) $R=0.3$, (b) $R=0.5$, (c) $R=0.65$, and (d) $R=0.7$ (units of g/s); remaining parameters and units of time intervals are the same as in Fig. 1.

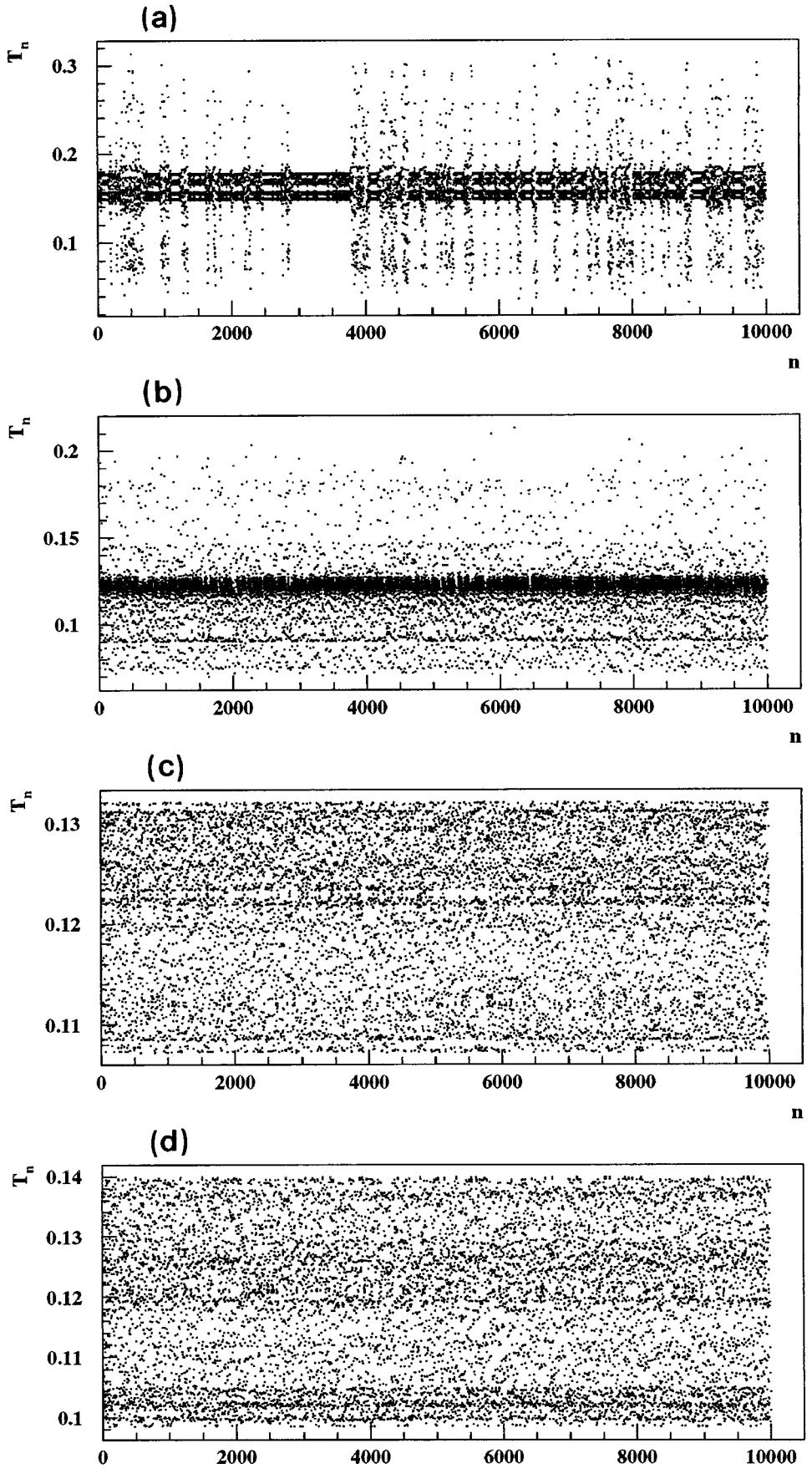

FIG. 5. Time series [T_n (s)] of drip intervals corresponding to attractors of Fig. 4 (n is the number of drops).

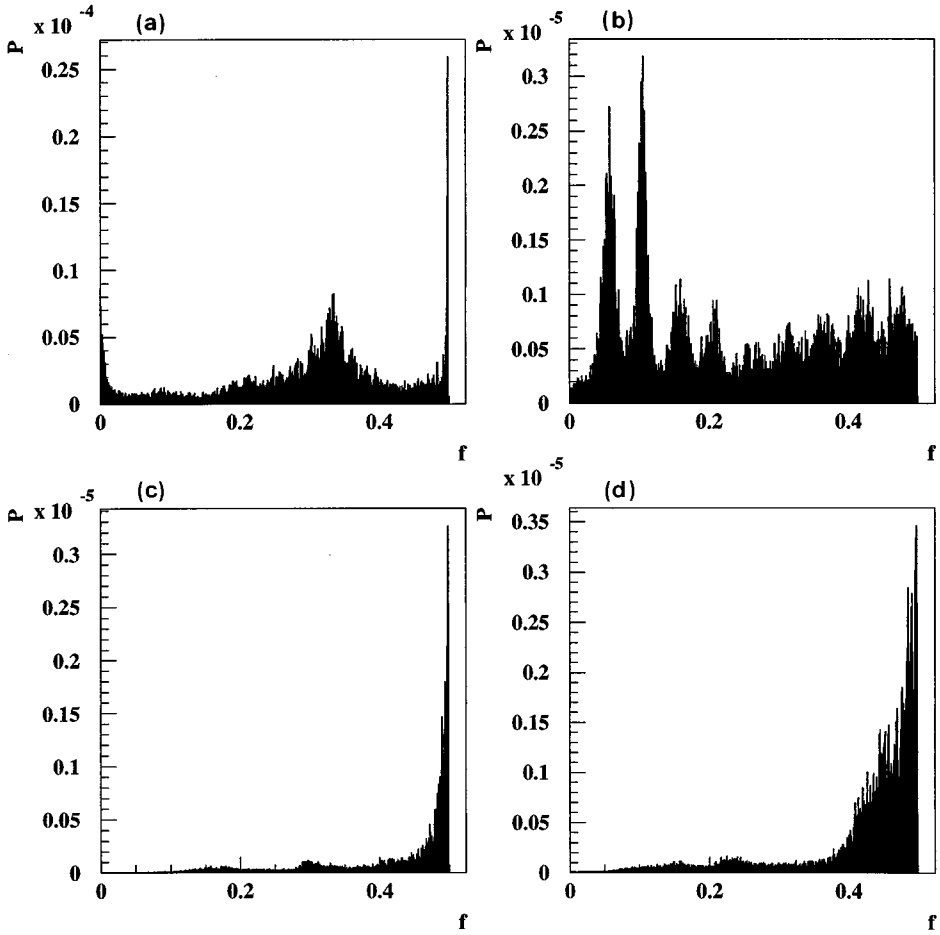

FIG. 6. Power spectra corresponding to the time series of Fig. 5 (units of f are drops^{-1}).

$$\frac{dx}{dt}=v,$$

$$\frac{d(Mv)}{dt}=Mg-kx-bv, \tag{1}$$

$$\frac{dM}{dt}=R,$$

where x is the coordinate of the center of mass of the forming drop, and R is the flow rate. The spring constant k represents surface tension, and b represents friction between the fluid and the faucet. When the drop position exceeds a threshold x_c, the mass M is suddenly reduced by an amount proportional to the speed of the drop, thus simulating the falling away of the drop.

As remarked by Bernhard [11], the nonlinearity required to yield chaos is the swift change at the threshold x_c. This change is represented by the release of mass of the drop and by the rebound of the residue water. In our models [13], and independently in the relaxation oscillator model of Ref. [12], the mass of the falling drop is supposed to be

$$\Delta M=\alpha M_c v_c, \tag{2}$$

where v_c is the speed and M_c the mass of the forming drop at the threshold x_c, and α is a parameter. This assumption is physically based and permits larger modifications and better control of parameters. Furthermore, by changing the initial position x_0 of each forming drop by an amount that depends on the mass of the falling drop, the rebound is enhanced, thus allowing the reproduction of a wide class of chaotic attractors, which present characteristics very similar to those determined experimentally.

Assuming the falling drop (of density ρ) to be spherical with radius $r=(3\Delta M/4\pi\rho)^{1/3}$, the rebound of the residue liquid can be modeled in a different way; in our previous studies (i) a pointlike residue is supposed, situated at the position $x_0=x_c-r\Delta M/M_c$ (*point-sphere* model); and (ii) a spherical residue of radius $r'=[3(M_c-\Delta M)/4\pi\rho]^{1/3}$ is left with its center at a distance $x_0=x_c-(r+r')\Delta M/M_c$ from the origin (*two-sphere* model).

The mechanism of detachment does not necessarily represent the actual behavior of the drop, and serves only to establish the initial conditions for the center of mass of the residue liquid after the break away of the drop and the following recoil. The present paper deals mainly with the numerical study of the point-sphere (PS) and two-sphere (TS) models, and a comparison of their features. These investigations are performed by calculating dripping spectra and time delay diagrams, with both mechanisms of rebound. Subse-

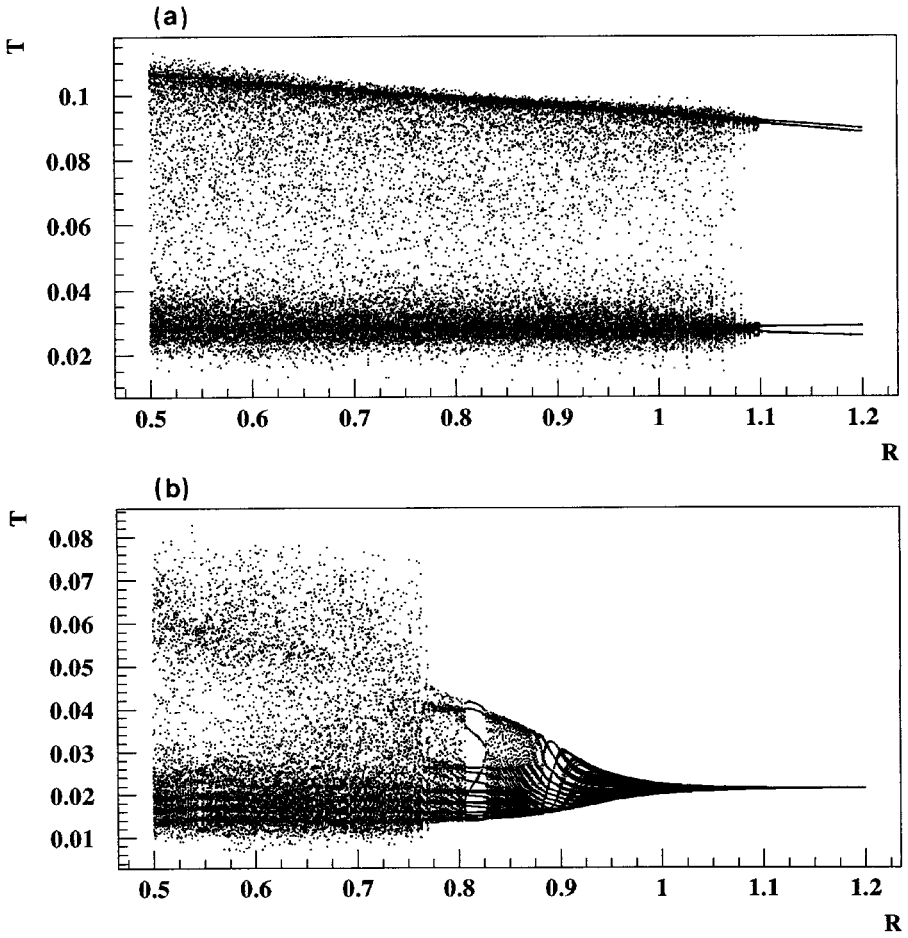

FIG. 7. TS dripping spectra [T (s)] plotted against flow rate R (g/s). The values of the parameters are the same of Fig. 1, but with (a) $\alpha=0.1$ s/cm and (b) $\alpha=0.05$ s/cm.

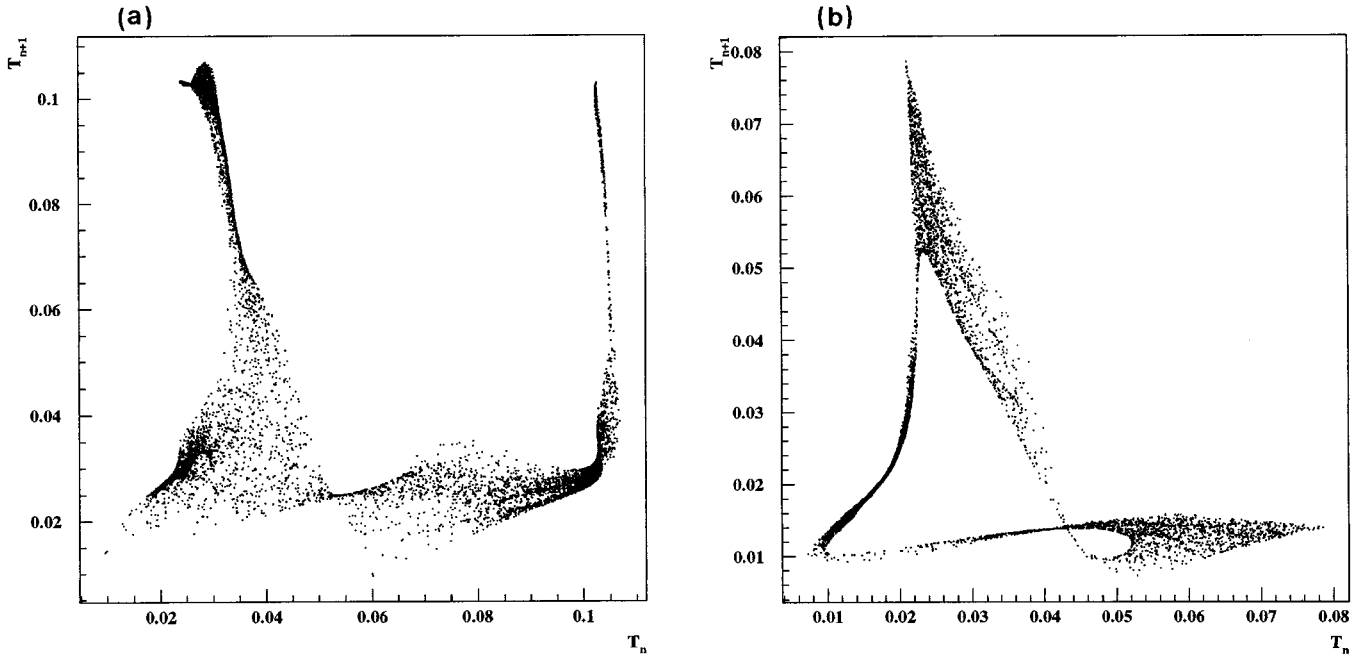

FIG. 8. Dripping patterns [T_n (s)] for the spectra of Figs. 7(a) and 7(b) at $R=0.65$ g/s, respectively.

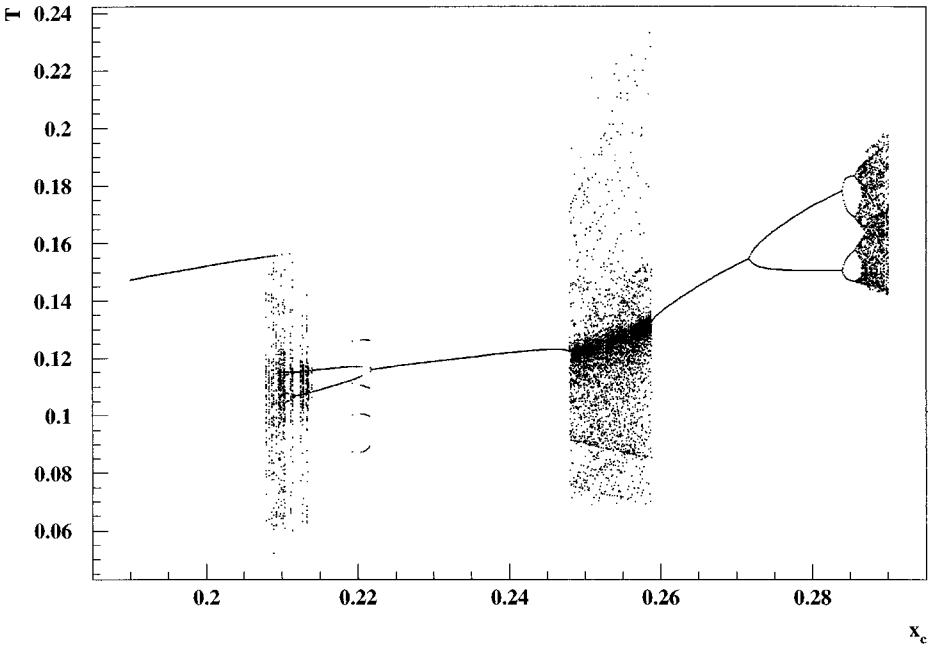

FIG. 9. PS bifurcation diagram [T (s)] obtained varying x_c (cm) at $R=0.5$ g/s; remaining parameters are as in Fig. 1.

quent variations of the physical parameters are performed, allowing an investigation of the dependence of the spectra upon the physical characteristics of the experimental apparatus. In fact, the model parameters have a correspondence with the physical characteristics (forms and dimensions) of the faucet and with the properties (density, cohesion and temperature) of the fluid. However, it should be observed that the number of independent parameters of models equations can be minimized [12,14]. Our analysis is thus performed allowing variations of the parameters k, α, and R (and only exceptionally x_c and b with the TS model).

Another paper [15] provided an analytical solution which substitutes the set of differential equations (1), reduces the computation time, and therefore speeds up an exhaustive exploration of the space of parameters. A subsequent work is in progress in order to carry out detailed investigations.

III. DRIPPING SPECTRA AND CHAOTIC ATTRACTORS

In order to reproduce the complex behavior of the dripping faucet, we calculated and recorded the time intervals T_n between successive drops by integrating numerically (see [13]) the differential equations (1) together with condition (2).

Dripping spectra, obtained by varying the flow rate R, are exhibited in Figs. 1 and 7 (throughout the paper the time interval unit is the second). For high values of the flux the integration cannot be continued, because in the simulation the falling of the drops becomes a continuous stream. Throughout, the acceleration due to gravity has been kept fixed at the value of $g=980$ cm/s^2. In Fig. 1 we plot the dripping spectrum obtained with the PS model, at values of parameters corresponding to water and typical eyedroppers. Inverse cascade, crisis, and chaotic behavior with periodic windows are visible. In Fig. 2, two successive enlargements of this spectrum around $R\simeq 0.5$ g/s show a transition from chaos to a period-1 attractor through tangent intermittence. Conversely, starting from $R\simeq 0.58$g/s, a period-doubling route to chaos is manifest. An enlargement of this last part of the spectrum is exhibited in Fig. 3, where a similarity between these features and those from chaos theory is clearly seen.

Inspection of Fig. 1, and the time-delay diagrams of Fig. 4, plotted at selected increasing values of R, show the capability of the model to exhibit a large variation of dynamics as the flow rate is varied. The plot of Fig. 4(a) and the corresponding time series diagram of Fig. 5(a) show periodic bands with bursts of chaos similar to those evidenced experimentally in the Figs. 12(a) and 12(b) of Ref. [9]. The power spectrum of Fig. 6(a) exhibits peaks in correspondence of frequencies $\frac{1}{2}$ and $\frac{1}{3}$. The attractor of Fig. 4(b) and the band with higher density in the corresponding time series diagram of Fig. 5(b) show a chaotic state characterized by a prevalence of time intervals around 0.12 s; the corresponding power spectrum, reported in Fig. 6(b), shows a dominance of frequencies around $\frac{1}{10}$ and $\frac{1}{20}$. The return map of Fig. 4(c) is very close to the ''parabola'' obtained experimentally in Ref. [3] and [6] and Fig. 4(d) shows that this attractor, by increasing R, undergoes stretching and folding, and discloses evidence of its own layered structure. The chaotic attractors of the region of Fig. 1 around $R\simeq 0.7$g/s have predominant frequencies with peaks around $\frac{1}{2}$, as is evident from the power spectra of Figs. 6(c) and 6(d).

In Fig. 7, spectra obtained with the TS model at the same values of parameters (except for α) of Fig. 1 are plotted. Figure 7(a), calculated with $\alpha=0.1$ s/cm, shows clearly a transition from chaos to period-4 behavior at $R\cong 1.1$g/s. A careful investigation of the corresponding return maps at different flow rates reveals that the variation of R produces generally small changes in the form of the attractor, an exception is the transition from chaotic to multiperiodic patterns. A different behavior appears at $\alpha=0.05$ s/cm, as

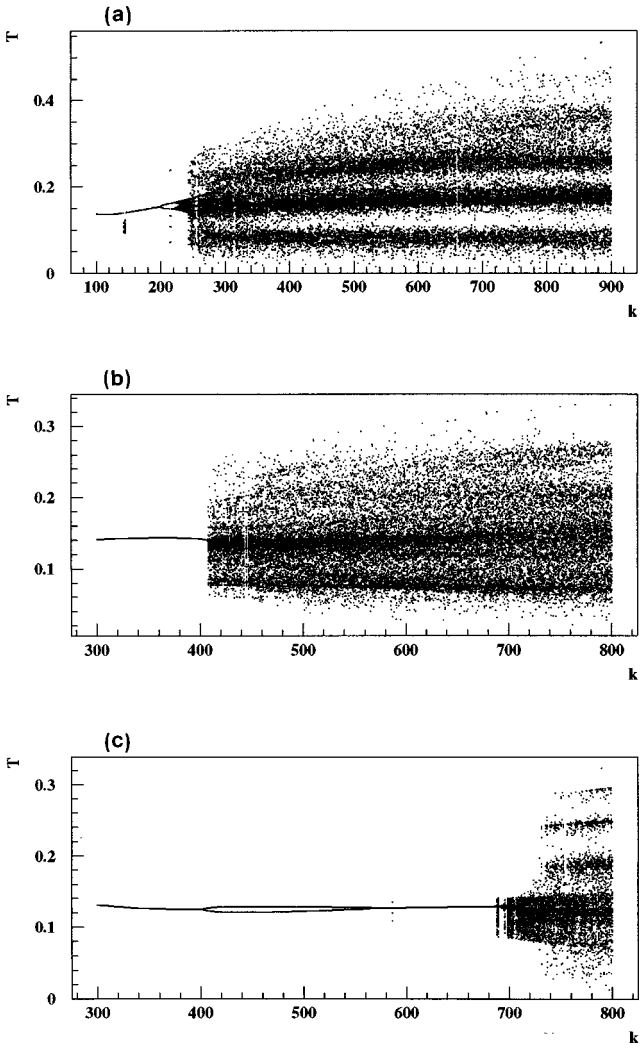

FIG. 10. Dripping spectra [T (s)] as a function of k dyn/cm at different values of the flow rate: (a) $R=0.2$, (b) $R=0.4$, and (c) $R=0.6$ (units of g/s). The remaining parameters are as in Fig. 1.

shown in Fig. 7(b): for increasing values of R an evolution from chaotic attractors to closed loops is displayed. However, apart from the appearance of periodic windows and closed loops, in this case the forms of strange attractors that can be obtained by varying R are also not substantially different. Return maps of Fig. 8 show typical chaotic attractors, relative to the two values of α considered, for $R=0.65$g/s.

In our studies, the TS model seems to present a weak dependence of the form of the chaotic attractors on the flow rate; however we will show in the following section that, on the contrary, by varying suitably k (and/or other parameters), a larger variety of strange attractors similar to the experimental ones is obtained.

IV. VARIATION OF PARAMETERS

A. Point-sphere model

Dripping time intervals versus x_c at $R=0.5$g/s are displayed in Fig. 9, where one can see period-1 regions separated from multiperiod and chaotic ones. Drawings of this type are useful in that they permit the singling out of bifurcation maps in R with different dynamical behaviors. However, we see no evidence of further advantages in varying x_c, as it is difficult to determine experimentally the point of release of the drop, which also depends on the conditions of equilibrium, and not only on the physical dimension and form of the nozzle. More interesting is the drawing of dripping time intervals as a function of the parameters R and k.

By varying the parameters R and k, we performed several calculations such as those shown in Fig. 10. One can observe an expected phenomenon: by increasing R, the region of chaoticity moves to larger values of surface tension in order to compensate for the increased effect of the gravitational force. The transitions from period-1 to chaotic states exhibited in the dripping spectra of Fig. 10 are different: in fact at low R we have a period-doubling pattern; increasing R further, we have a crisis, whereas a particular behavior is shown at $R=0.6$g/s, where the spectrum evolution occurs through cycle-limit patterns at $k\simeq 700$ dyn/cm, not evident on the figure because of its scale. Evidence of such a type of transition is shown in the plot of four return maps, reported in Fig. 11. At large k the states seem to be characterized by the presence of bands of time drop intervals. Reduction of k produces, globally, a less diffuse dynamical behavior, as one can see observing the spectra of Fig. 12 and the attractors of Fig. 13 [compare with the attractors of Figs. 4(a) and 4(c)].

B. Two-sphere model

From the TS spectrum of Fig. 14 [obtained by varying x_c, maintaining the same values of the parameters of the spectrum of Fig. 7(a) and for $R=0.9$g/s], one deduces that, apart from the transition to a period-1 attractor at $x_c\simeq 0.49$ cm, no significant changes in the form of the attractors are seen. Conversely, by varying the values of the parameter k, one obtains the bifurcation diagram of Fig. 15 (here $r=0.9$g/s and $x_c=0.25$ cm). This spectrum exhibits periodic windows and crisis. We have investigated the region ranging from $k\cong 300$ dyn/cm to $k\cong 330$ dyn/cm which shows an interesting dynamical behavior. In this part of the spectrum we have selected four values of the parameter k, and in Fig. 16 we report the corresponding return maps. As we can see from these delay diagrams, the spectrum exhibits continuous transitions from the period-1 states [Fig. 16(a)], through the development of a loop [Figs. 16(b) and 16(c)], to a sequence of chaotic patterns leading to the state of Fig. 16(c). This transition is initiated by distortion of the loop of Fig. 16(b) in three corners, followed by stretching and folding which lead to chaotic attractors. As is also demonstrated experimentally [5], here we find that the lowering of the surface tension produces large changes in the dynamics, and reveals the existence of closed-loop states. As we already showed above, the return maps of Fig. 11 have an analog in the behavior for PS models but at high-k values. However, it should be noted that such transition happens for TS models at lower R values, compensating in some way for the effect of smaller liquid surface tension.

We must observe that, for TS models, a decrease in α can also produce, in limited regions, almost the same effect of a suitable reduction in k, as can be deduced by inspection of Fig. 7(b). This phenomenon can be understood by observing

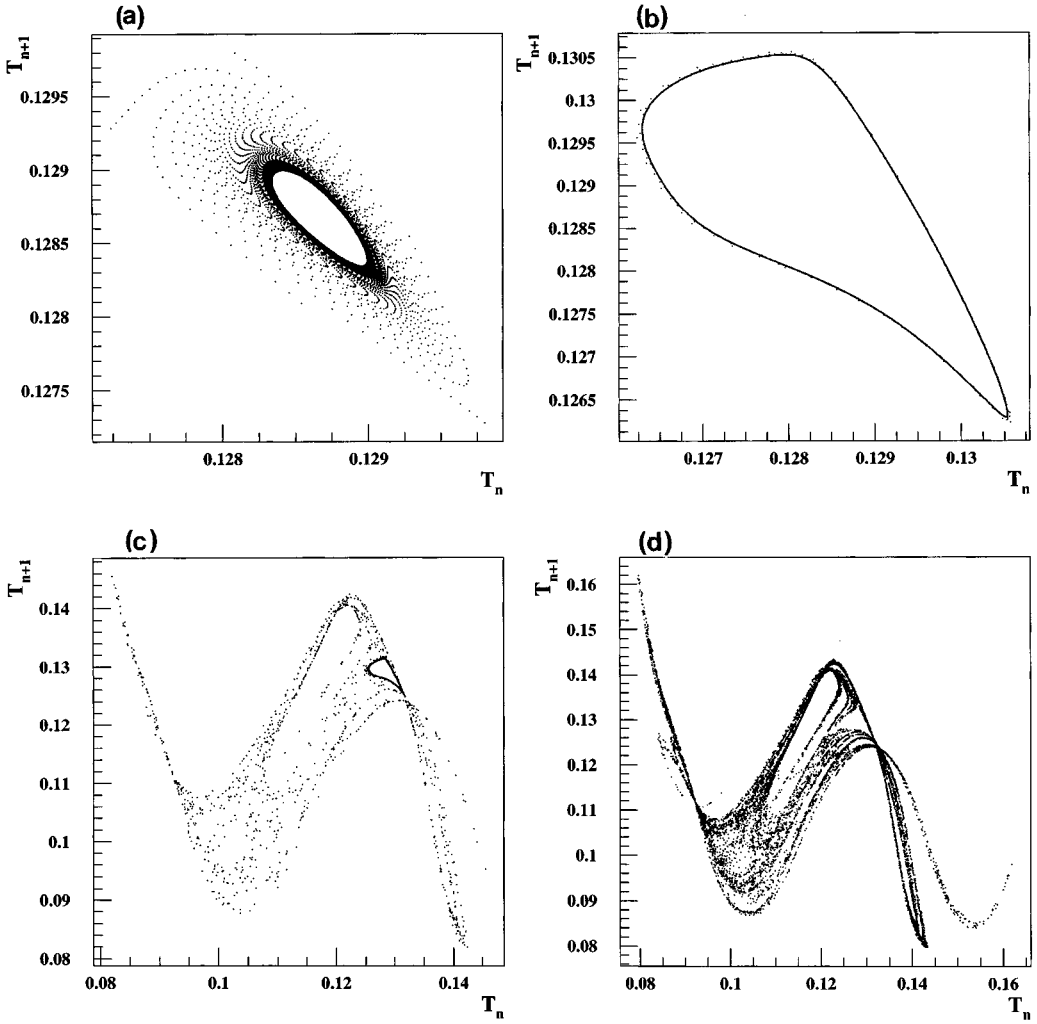

FIG. 11. Time delay [T_n. (s)] diagrams at $R=0.6$ g/s [from the spectrum of Fig. 10(c)] and (a) $k=700$, (b) $k=705$, (c) $k=710$, and (d) $k=720$ (units dyn/cm). When increasing k, a transition from a limit cycle to chaotic attractors is clearly seen.

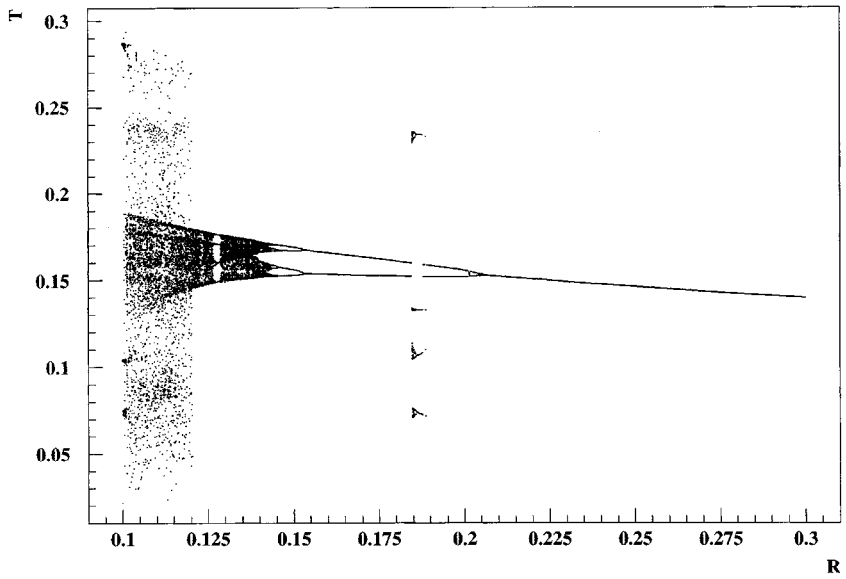

FIG. 12. Bifurcation diagram [T (s)] as a function of R (g/s) at $k=200$ dyn/cm. Parameters are as in Fig. 1.

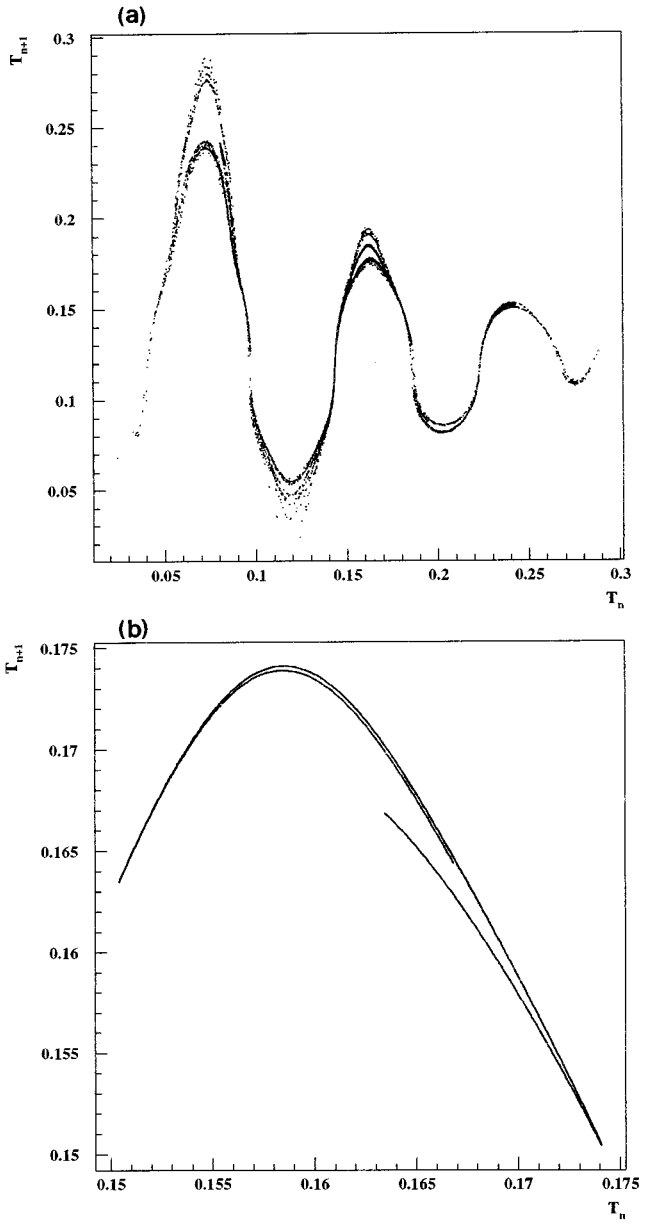

FIG. 13. Return maps [T_n (s)] from the bifurcation diagram of Fig. 12 at (a) $R=0.11$ g/s and (b) $R=0.135$ g/s.

that decreasing the depletion of M has an effect equivalent to reduction of the restoring force. In addition, a reduction of α or k can compensate for the larger rebound of TS models with respect to PS models, thus re-establishing a variety in the model dynamics. As a consequence α seems to be linked somehow to k.

Guided by previous results, we investigated the effects due to large variations of k, and b and x_c. For most of the domain of parameters investigated, the system shows the presence of chaotic attractors. The dripping spectrum for $k=1500$ dyn/cm, $b=3.3$g/s, $x_c=0.98$ cm, and $\alpha=0.34$ s/cm is shown in Fig. 17. Two enlargements, reported in Fig. 18, show the regions where the sudden changes of dynamical behavior of the faucet occur.

We found that by varying the flow rate R the system exhibits attractors which reproduce the complexity of some experimental data [3–6,9]. For the sake of brevity, in Fig. 19 return maps relative only to two of the many cases analyzed are reported. Besides the attractor plotted in Fig. 19(a), which reveals clearly its fractal structure, in Fig. 19(b) we show a quaint attractor, which presents itself as a set of ''islets,'' surrounded with a ''cloud'' of erratic points (these closed loops are similar to those of Fig. 8(b) of Ref. [5]).

V. REPRODUCING EXPERIMENTAL ATTRACTORS

As remarked previously, the PS model demonstrates a dependence on the flow rate and spectra which show patterns very similar to those found experimentally [5]. In Fig. 20 we display a bifurcation diagram obtained with the PS model at a value of the surface tension significantly smaller than that of water: as one can see, this spectrum starting from periodic attractors, presents a rich variety of transitions to chaos and then, at large values of R, a jump to a period-1 attractor, passing through periodic and strange attractors and showing intermittence, crisis, gap, etc.

In order to make a comparison between our experimental results and model predictions, we have measured and recorded dripping intervals using a typical leaky faucet experimental apparatus. In Fig. 21, attractors obtained experimentally by using an aqueous solution [16] are compared with return maps calculated from the spectrum of Fig. 20 at two selected flow rates: as one can clearly see, the similarity between the attractors is remarkable. The corresponding power spectra are reported respectively in Fig. 22, where we can observe that plots (c) and (d) reveal an impressive resemblance, whereas plots (a) and (b) show peak frequencies near to $\frac{1}{2}$ and $\frac{1}{3}$, respectively. As far as we know, analogous reproductions have not been obtained before now.

VI. CONCLUSIONS

The present and previous studies show that the description of the dynamics of the dripping faucet with a relaxation oscillator model presents a great variety of behaviors, included closed-loop patterns. The analyses presented in this paper demonstrate that both models proposed have a good qualitative agreement with the behavior of the actual dripping faucet. It is shown that with the use of the PS model one is able to produce spectra, at various values of the flow rate R, with characteristics that have many experimental counterparts in the real system. Allowing a large variation of the parameters one can observe that the TS model is also capable, in some cases, of reproducing features of attractors obtained experimentally with fluids of low surface tension. Some observations must be made. It seems rather clear to us that irregularities in the dynamics are characteristic of any relaxation oscillator with unexpected change and rebound at the threshold. Thus dripping faucet models differ in the mechanism which simulates the detachment of the drops. So far, we believe that the PS model has, with respect to the other models present in the literature, a larger richness of features which better reproduce the experimental data. The reason is that the PS model (or TS model), after the falling of a drop, merely sets the residual liquid at a higher upward position, thus enhancing the rebound. The results presented in this paper suggest that the complexity of the dynamics of the

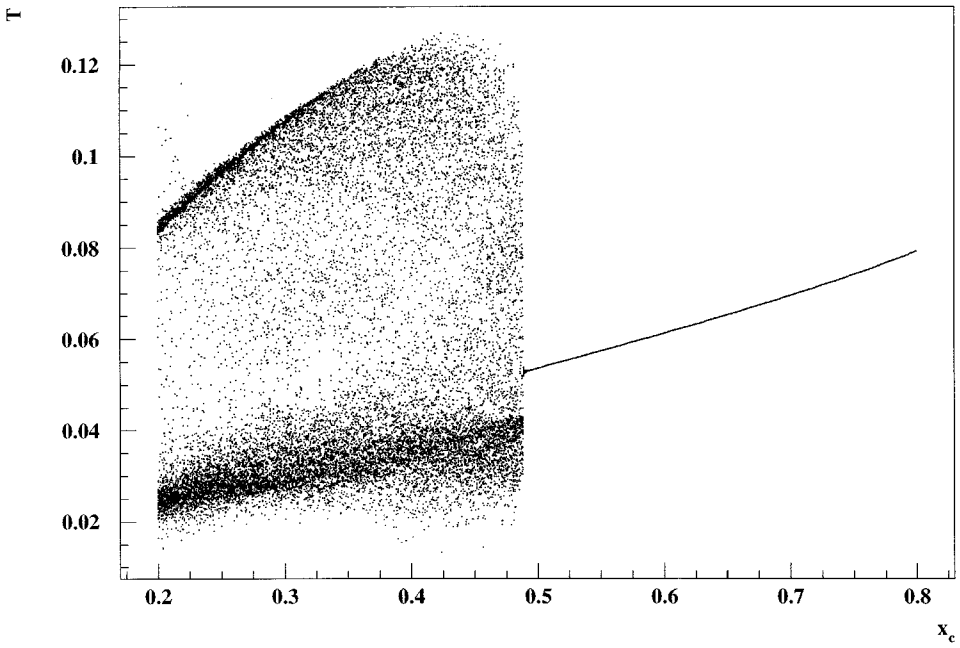

FIG. 14. TS dripping spectrum [T (s)] as a function of the critical distance x_c (cm) at $R=0.90$ g/s. Other parameters are the same as in Fig. 7(a).

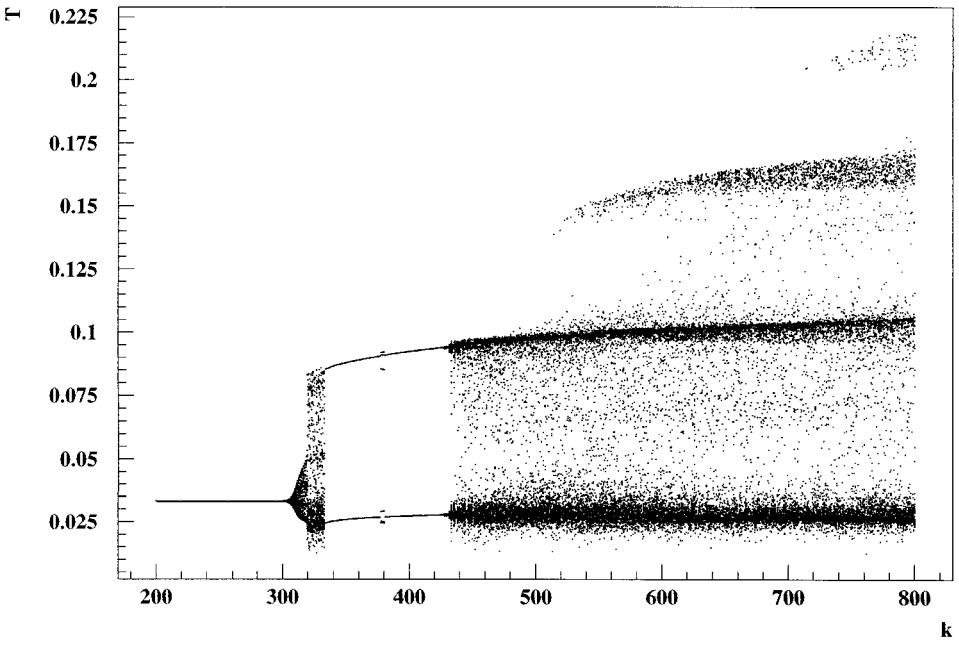

FIG. 15. Dripping spectrum [T (s)] as a function of the parameter k dyn/cm at $R=0.90$ g/s and $x_c=0.25$ cm. Other parameters are the same as in Fig. 7(a).

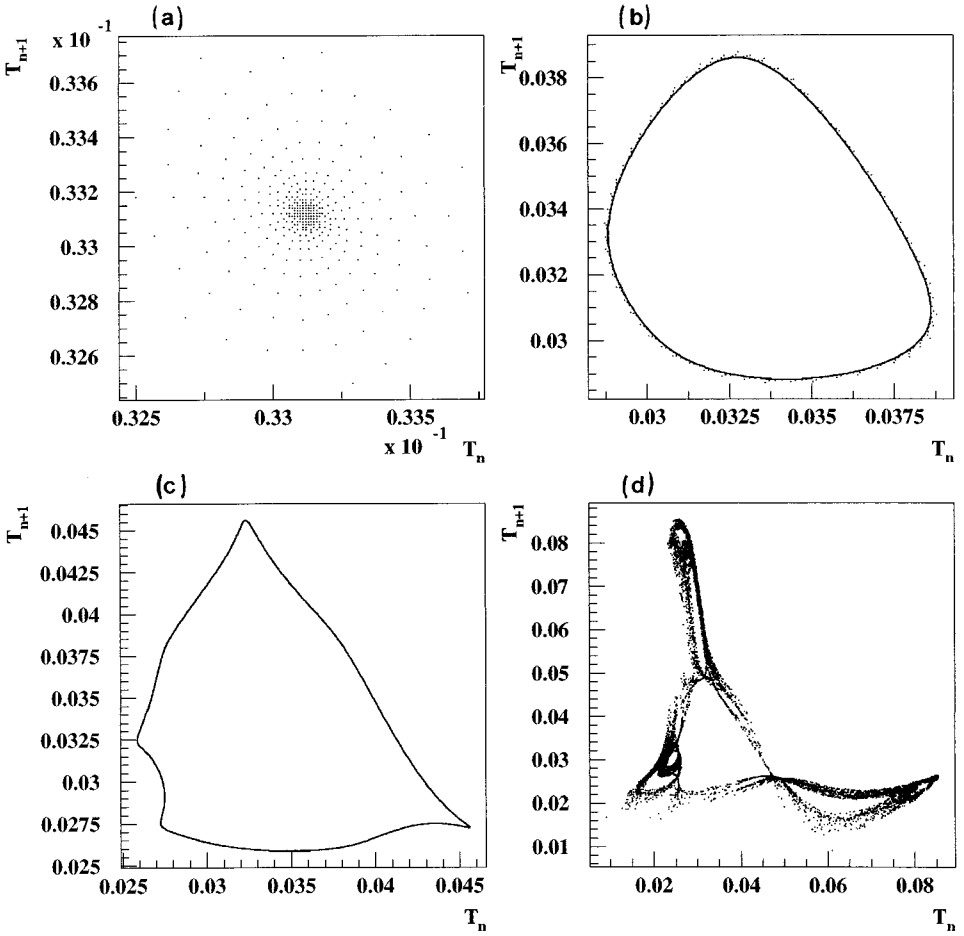

FIG. 16. Four discrete time return maps [T_n (s)] of the dripping spectrum of Fig. 15: (a) $k=305$, (b) $k=310$, (c) $k=315$, and (d) $k=325$ (units dyn/cm).

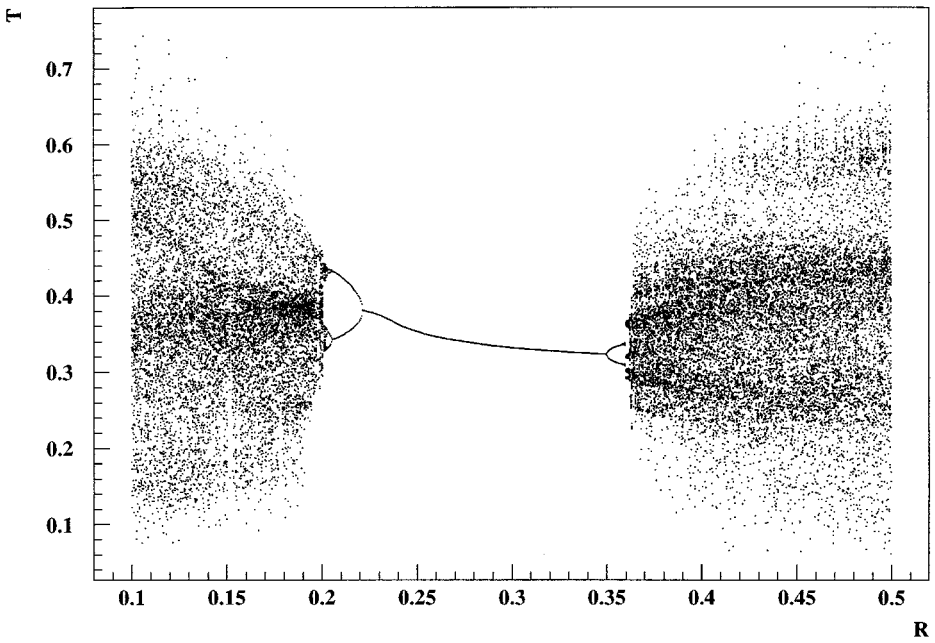

FIG. 17. Dripping spectrum [T (s)] as a function of R (g/s). The values of the parameters are: $g=980$ cm/s^2, $x_c=0.98$ cm, $k=1500$ dyn/cm, $b=3.3$ g/s, and $\alpha=0.34$ s/cm.

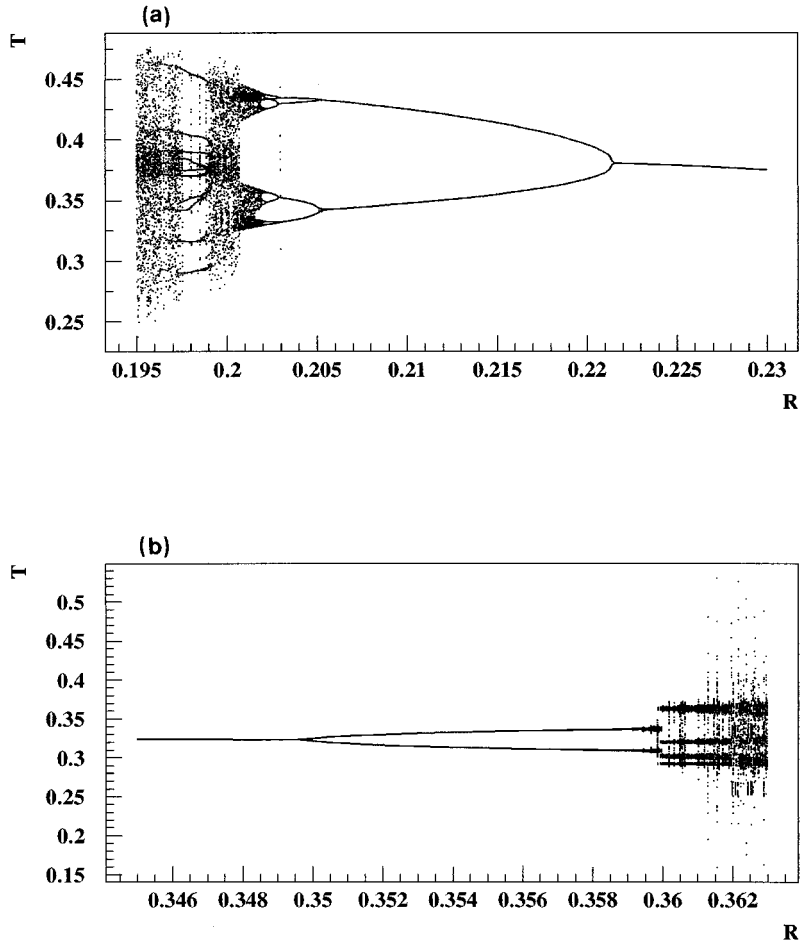

FIG. 18. Two region enlargements of the spectrum of Fig. 17 (units as in Fig. 17).

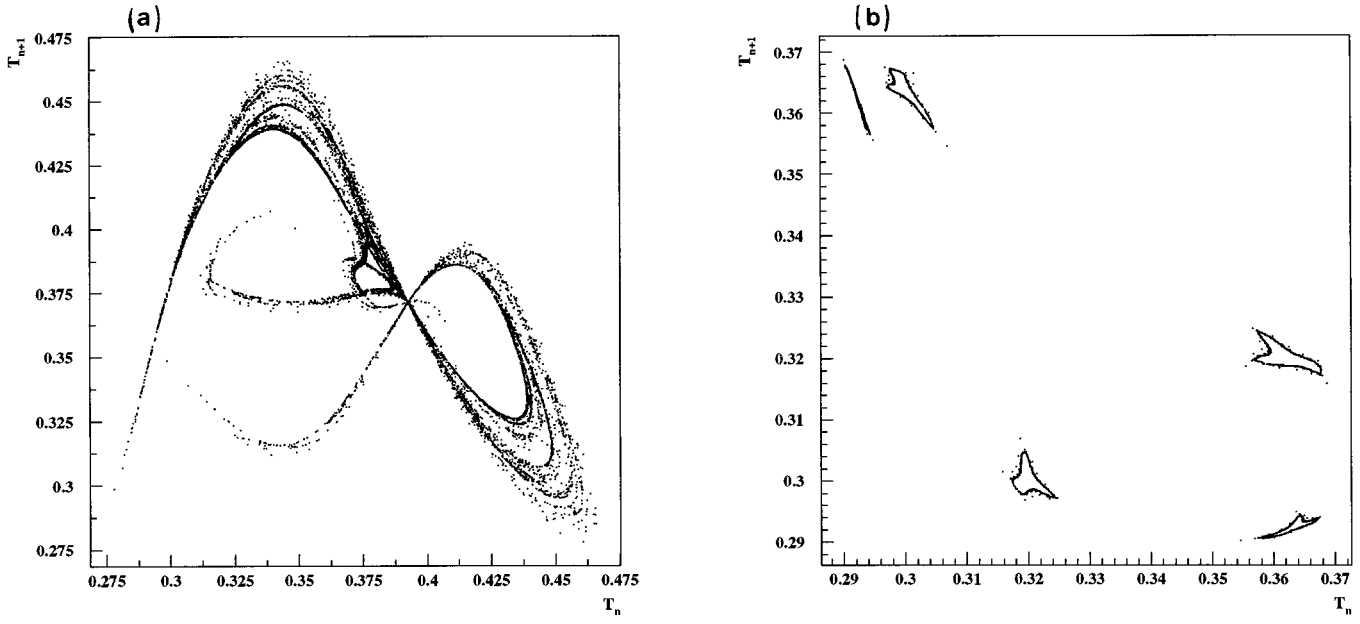

FIG. 19. Dripping time [T_n (s)] delay diagrams from the spectrum of Fig. 17 at (a) $R=0.2$ g/s and (b) $R=0.362$ g/s.

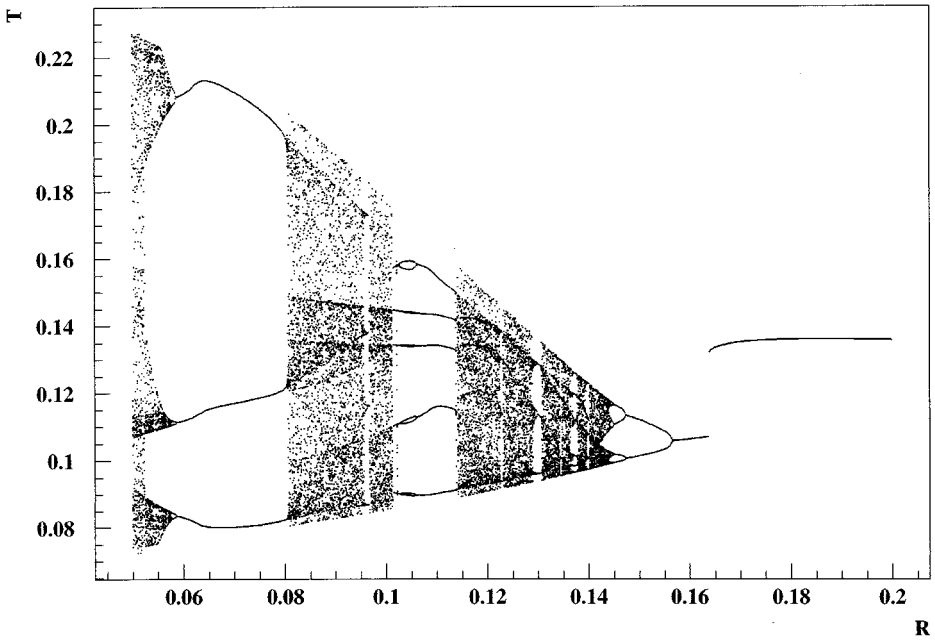

FIG. 20. PS bifurcation diagram [T (s)] as function of R (g/s) at $k=120$ dyn/cm. Parameters are as in Fig. 1.

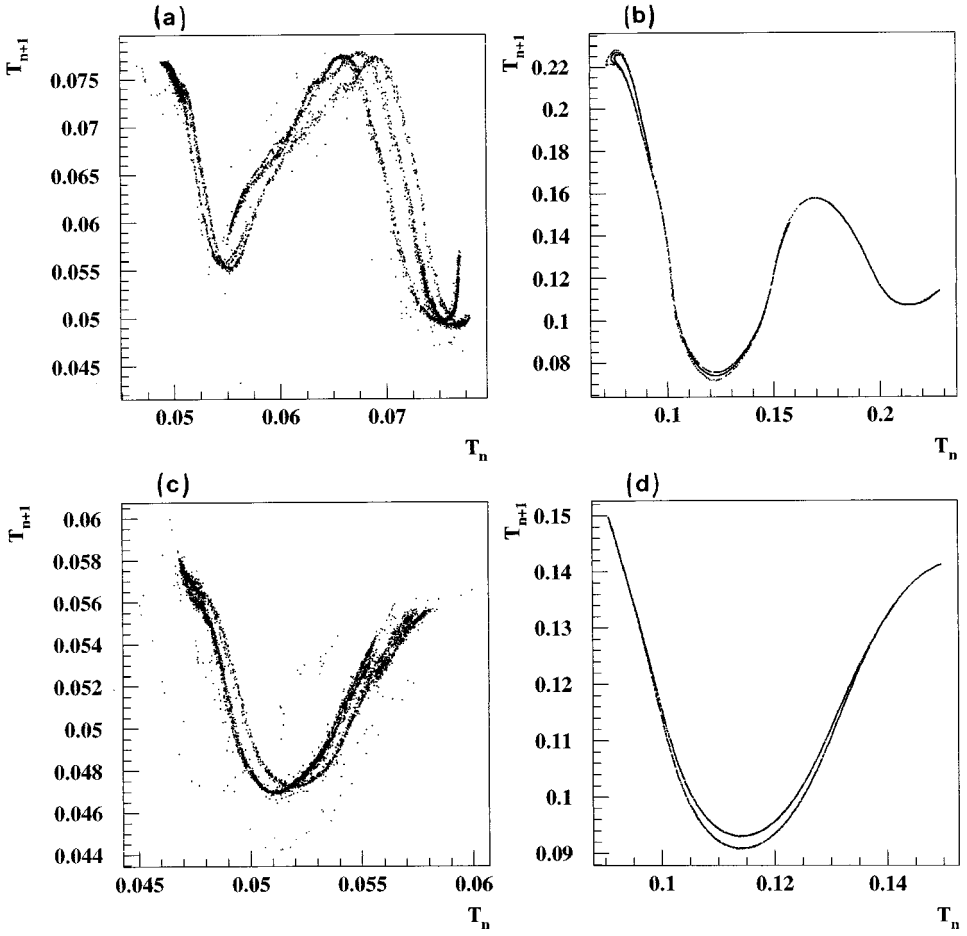

FIG. 21. Comparison between experimental and PS attractors [T_n (s)]. (a) Experimental attractor for an aqueous solution of surface tension $\tau\simeq 36$ dyn/cm at $R\simeq 0.57$ g/s for a brass nozzle with an inner diameter of 0.2 cm and an outer diameter of 0.4 cm. (b) Return map from the dripping spectrum of Fig. 19 at $R=0.05$ g/s. (c) Experimental attractor for the same solution at $R\simeq 0.61$ g/s. (d) Return map at $R=0.12$ g/s.

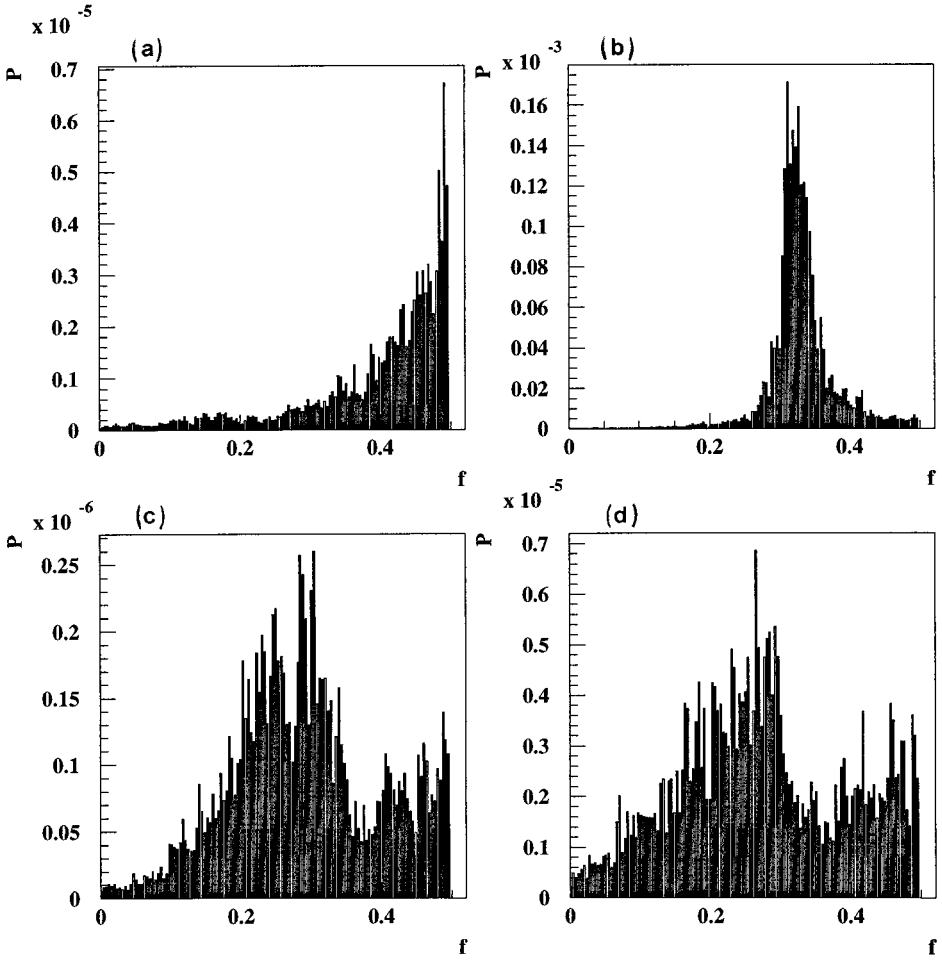

FIG. 22. Power spectra relative to the delay diagrams of Fig. 21 (units as in Fig. 6).

dripping faucet can be understood if the mechanism at the critical point is analyzed more deeply.

We are aware that the state of the research is still far from furnishing precise answers, but we believe that the possibility of exhaustive investigations, provided by the use of analytical solutions [15], can produce more detailed explanations.

ACKNOWLEDGMENTS

It is a pleasure to thank P. Rotelli for useful remarks and discussions.

[1] O. E. Rössler, in *Synergetics: A Workshop*, edited by H. Haken (Springer, Berlin, 1977), p. 174.
[2] R. S. Shaw, *The Dripping Faucet as a Model Chaotic System* (Aerial, Santa Cruz, 1984).
[3] P. Martien, S. C. Pope, P. L. Scott, and R. S. Shaw, Phys. Lett. **110A**, 399 (1985).
[4] H. N. Núñez Yépez, A. L. Salas Brito, C. A. Vargas, and L. A. Vicente, Eur. J. Phys. **10**, 99 (1989).
[5] X. Wu, E. Tekle, and Z. A. Schelly, Rev. Sci. Instrum. **60**, 3779 (1989); X. Wu and Z. A. Schelly, Physica D **40**, 433 (1989).
[6] R. F. Cahalan, H. Leidecker, and G. D. Calahan, Comput. Phys. **4**, 368 (1990).
[7] K. Dreyer and F. R. Hickey, Am. J. Phys. **59**, 619 (1991).
[8] J. Austin, Phys. Lett. A **155**, 148 (1991).
[9] J. C. Sartorelli, W. M. Gonçalves, and R. D. Pinto, Phys. Rev. E **49**, 3963 (1994).
[10] Z. Néda, B. Bakó, and E. Rees, Chaos **6**, 59 (1996).
[11] P. A. Bernhardt, Physica D **52**, 489 (1991).
[12] G. I. Sánchez-Ortiz and A. L. Salas-Brito, Phys. Lett. A **203**, 300 (1995); G. I. Sánchez-Ortiz and A. L. Salas-Brito, Physica D **89**, 151 (1995).
[13] A. D'Innocenzo and L. Renna, Int. J. Theor. Phys. **35**, 941 (1996).
[14] G. I. Sánchez-Ortiz, Senior thesis, FCUNAM, D. F. Mexico, 1991.
[15] A. D'Innocenzo and L. Renna, Phys. Lett. A **220**, 75 (1996).
[16] F. Giannelli, Ph.D. thesis, Dip. di Fisica, Università di Lecce, Italy, 1995.